

# Nucleon form factors at threshold

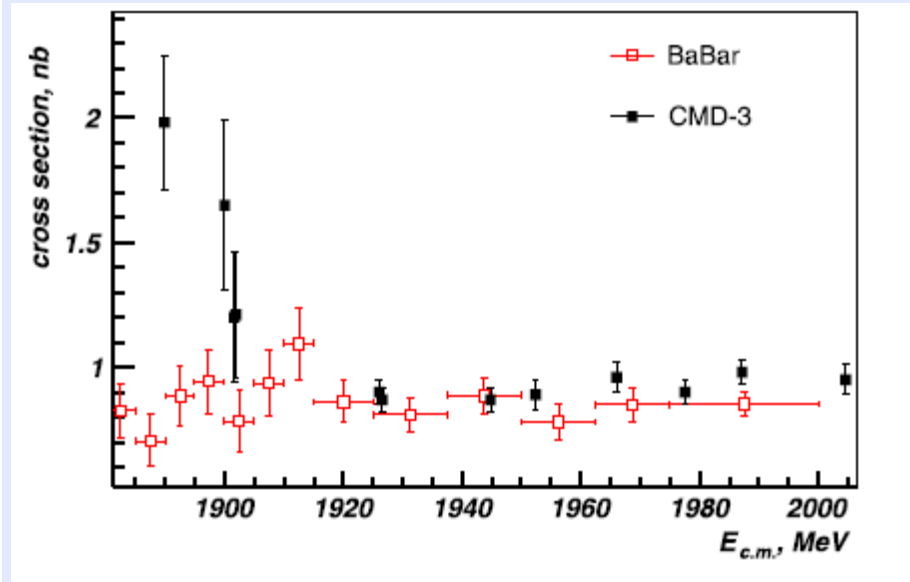
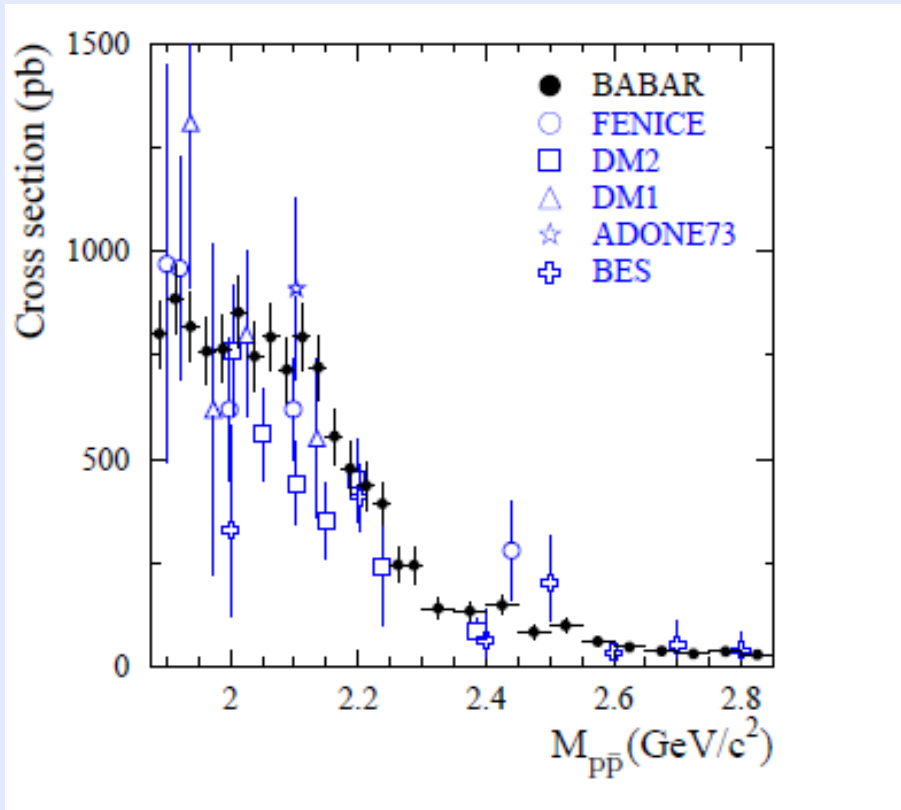
A.I. Milstein

G.I.Budker Institute of Nuclear Physics, Novosibirsk, Russia

## Layout

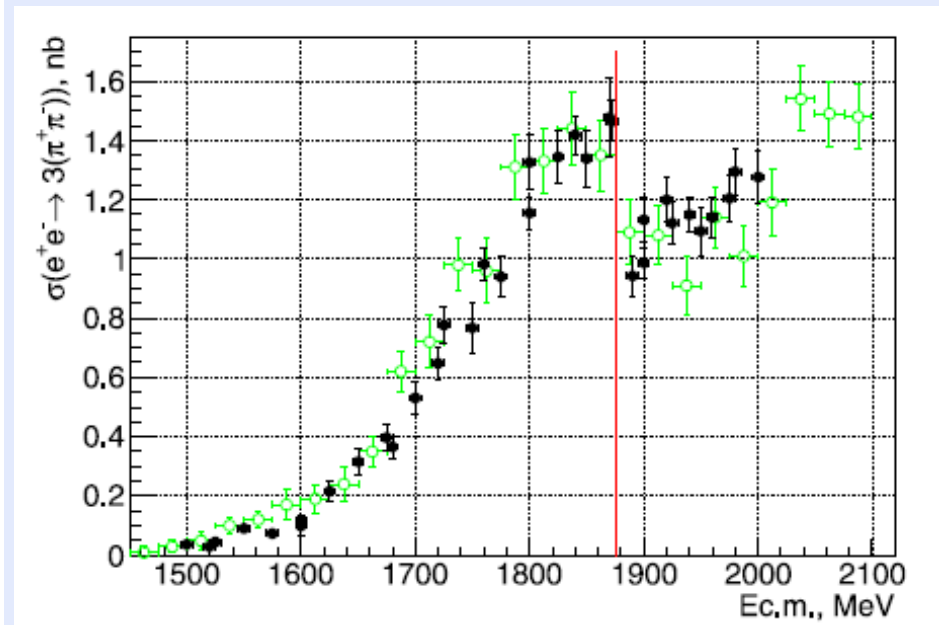
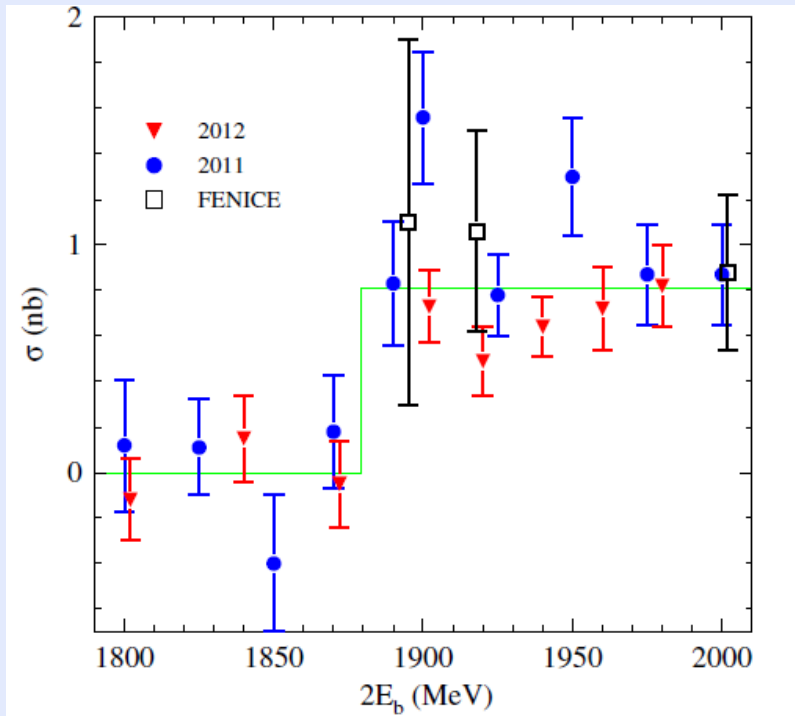
- Cross sections  $e^+e^- \rightarrow p\bar{p}, n\bar{n}, 3(\pi^+\pi^-), 2(\pi^+\pi^-\pi^0)$ .
- Optical potentials.
- The amplitude of  $e^+e^- \rightarrow N\bar{N}$  near the threshold.
- Structure of the wave functions,  $G_E, G_M$ .
- Predictions for the cross section of  $e^+e^- \rightarrow N\bar{N}$  and  $G_E/G_M$ .
- Virtual  $N\bar{N}$  pair production near the threshold.
- Predictions for  $e^+e^- \rightarrow 6\pi$ .
- Angular distributios in  $J/\psi \rightarrow p\bar{p}\pi^0(\eta)$  decays.
- $J/\psi \rightarrow p\bar{p}\rho(\omega)$  decays
- $J/\psi, \psi(2S) \rightarrow p\bar{p}\gamma$  decay.
- $J/\psi \rightarrow \gamma\eta'\pi^+\pi^-$  decay.
- Conclusion.

$e^+e^- \rightarrow p\bar{p}$ , near the threshold of the process,  
strong energy dependence!



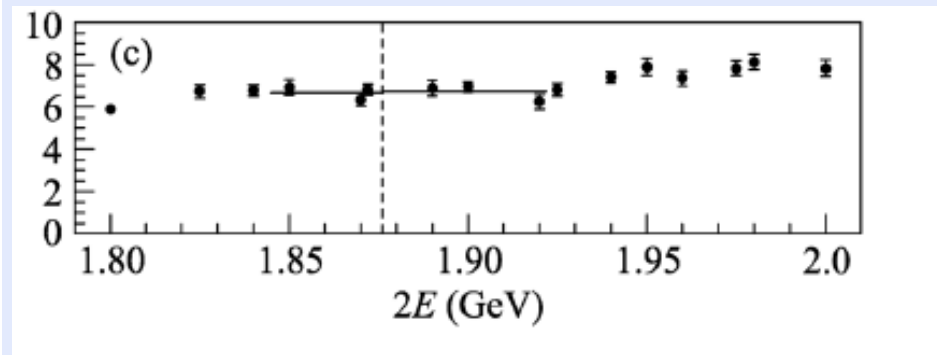
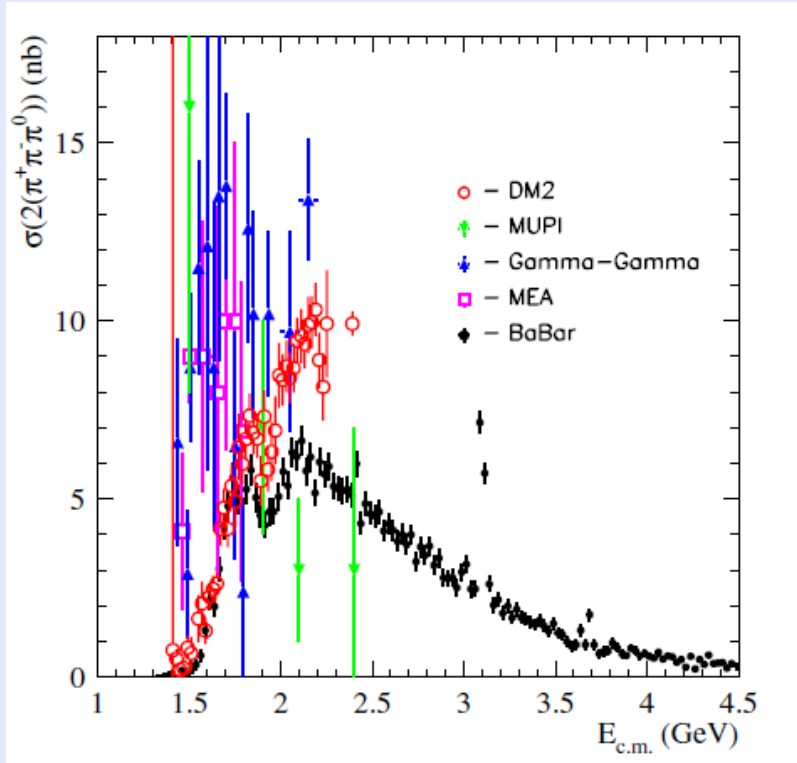
**Cross section  $e^+e^- \rightarrow p\bar{p}$ ; Left picture:** data are from B. Aubert, et al., BaBar, Phys. Rev. D 73, 012005 (2006); **right picture:** R.R.Akhmetshin, et al., CMD3, Physics Letters B759, 634 (2016), J.P. Lees, et al., BaBar, Phys. Rev. D 87 (2013) 092005

# $e^+e^- \rightarrow n\bar{n}, 3(\pi^+\pi^-)$ near the threshold of $N\bar{N}$ pair production



Left picture: cross section  $e^+e^- \rightarrow n\bar{n}$ ; data are from M.N. Achasov, et al., SND, Phys. Rev. D 90, 112007 (2014); right picture: cross section  $e^+e^- \rightarrow 3(\pi^+\pi^-)$ ; data are from R.R.Akhmetshin, et al., CMD3, Physics Letters, B723, 634 (2013), (black dots); B. Aubert, et al., BaBar, Phys. Rev. D 73 (2006) 052003, (green open circles)

$e^+e^- \rightarrow 2(\pi^+\pi^-\pi^0)$  and a sum of the cross sections  $e^+e^- \rightarrow 6\pi$  and  $e^+e^- \rightarrow N\bar{N}$  near the threshold of  $N\bar{N}$  pair production



Left picture: cross section  $e^+e^- \rightarrow 2(\pi^+\pi^-\pi^0)$ ; data are from B. Aubert, et al., BaBar , Phys. Rev. D 73 (2006) 052003; right picture: a sum of cross sections  $e^+e^- \rightarrow N\bar{N}$  and  $e^+e^- \rightarrow 6\pi$ ; data are from A.E. Obrazovsky and S.I. Serednyakov, JETP letters 99 (2014) 315. There is no evidence of a structure in the total cross section!

Strong enhancement of decay probability at low invariant mass of  $p\bar{p}$  in the processes  $J/\Psi \rightarrow \gamma p\bar{p}$ ,  $B^+ \rightarrow K^+ p\bar{p}$  and  $B^0 \rightarrow D^0 p\bar{p}$ ,  $B^+ \rightarrow \pi^+ p\bar{p}$  and  $B^+ \rightarrow K^0 p\bar{p}$ ,  $\Upsilon \rightarrow \gamma p\bar{p}$ ... These effects are similar to that in  $e^+e^-$  annihilation.

One of the most natural explanation of this enhancement is final state interaction of nucleon and antinucleon

B. Kerbikov, A. Stavinsky, and V. Fedotov, Phys. Rev. C **69**, 055205 (2004); D.V. Bugg, Phys. Lett. B **598**, 8 (2004); B. S. Zou and H. C. Chiang, Phys. Rev. D **69**, 034004 (2004); B. Loiseau and S. Wycech, Phys. Rev. C **72**, 011001 (2005); A. Sibirtsev, J. Haidenbauer, S. Krewald, Ulf-G. Meiner, and A.W. Thomas, Phys. Rev. D **71**, 054010 (2005); J. Haidenbauer, Ulf-G. Meiner, A. Sibirtsev, Phys.Rev. D **74**, 017501 (2006); V.F. Dmitriev and A.I.Milstein, Phys. Lett. B **658** (2007), 13.

## Final state interaction

Final state interaction (including annihilation channels) may be taken into account by means optical potentials:

$$V_{N\bar{N}} = U_{N\bar{N}} - iW_{N\bar{N}}.$$

Nijmegen, Paris, Jülich... optical potentials give the same predictions for the cross sections of elastic and inelastic scattering of unpolarized particles but **essentially different predictions for spin observables!**

The cross section  $\sigma = \sigma_{ann} + \sigma_{cex} + \sigma_{el}$  of  $p\bar{p}$  scattering has the form

$$\sigma = \sigma_0 + (\zeta_1 \cdot \zeta_2) \sigma_1 + (\zeta_1 \cdot \nu)(\zeta_2 \cdot \nu) (\sigma_2 - \sigma_1),$$

where  $\zeta_1$  and  $\zeta_2$  are the unit polarization vectors of the proton and antiproton, respectively.

**Investigation of the process  $e^+e^- \rightarrow N\bar{N}$  gives important information for modification of optical potentials!**

## The amplitude of $e^+e^- \rightarrow N\bar{N}$ near the threshold

In the non-relativistic approximation the amplitude  $T_{\lambda\mu}^I$  in units  $4\pi\alpha/Q^2$  for the certain isospin channel  $I = 0, 1$  reads (V.F.Dmitriev, A.I.Milstein, S.G.Salnikov, Phys.At.Nucl. 77, 1173 (2014)):

$$T_{\lambda\mu}^I = G_s^I \left\{ \sqrt{2}u_{1R}^I(0)(\mathbf{e}_\mu \cdot \boldsymbol{\epsilon}_\lambda^*) + u_{2R}^I(0) \left[ (\mathbf{e}_\mu \cdot \boldsymbol{\epsilon}_\lambda^*) - 3(\hat{\mathbf{k}} \cdot \mathbf{e}_\mu)(\hat{\mathbf{k}} \cdot \boldsymbol{\epsilon}_\lambda^*) \right] \right\},$$

where  $G_s^I$  is an energy-independent constant,  $\mathbf{e}_\mu$  is a virtual photon polarization vector, corresponding to the projection of spin  $J_z = \mu = \pm 1$ ,  $\boldsymbol{\epsilon}_\lambda$  is the spin-1 function of  $N\bar{N}$  pair,  $\lambda = \pm 1, 0$  is the projection of spin on the nucleon momentum  $\mathbf{k}$ , and  $\hat{\mathbf{k}} = \mathbf{k}/k$ .

The Hamiltonian  $H^I$  of  $N\bar{N}$  interaction for the isospin  $I$  is

$$H^I = \frac{p_r^2}{M} + V_S^I(r)\delta_{L0} + V_D^I(r)\delta_{L2} + V_T^I(r) S_{12},$$

$$S_{12} = 6(\mathbf{S} \cdot \mathbf{n})^2 - 4,$$

where  $\mathbf{S}$  is the spin operator for the spin-one system of the produced pair,  $L$  denotes the orbital angular momentum, and  $\mathbf{n} = \mathbf{r}/r$ .



## Radial wave functions

The radial wave functions  $u_{nR}^I(r)$  and  $w_{nR}^I(r)$ ,  $n = 1, 2$ , are the regular solutions of the equations

$$\frac{p_r^2}{M}\chi_n + \mathcal{V}\chi_n = 2E\chi_n,$$

$$\mathcal{V} = \begin{pmatrix} V_S^I & -2\sqrt{2}V_T^I \\ -2\sqrt{2}V_T^I & V_D^I - 2V_T^I + \frac{6}{Mr^2} \end{pmatrix}, \quad \chi_n = \begin{pmatrix} u_n^I \\ w_n^I \end{pmatrix}.$$

Here  $M$  is the proton mass,  $E = k^2/(2M)$ . The asymptotic forms of the regular solutions at large distances are

$$u_{1R}^I(r) = \frac{1}{2ikr} \left[ S_{11}^I e^{ikr} - e^{-ikr} \right], \quad w_{1R}^I(r) = -\frac{1}{2ikr} S_{12}^I e^{ikr},$$

$$u_{2R}^I(r) = \frac{1}{2ikr} S_{21}^I e^{ikr}, \quad w_{2R}^I(r) = \frac{1}{2ikr} \left[ -S_{22}^I e^{ikr} + e^{-ikr} \right],$$

where  $S_{21}^I = S_{12}^I$ ,  $|S_{11}^I|^2 + |S_{12}^I|^2 \leq 1$ , and  $|S_{22}^I|^2 + |S_{21}^I|^2 \leq 1$ .

## The cross section of $e^+e^- \rightarrow N\bar{N}$ near the threshold

The cross section reads

$$\frac{d\sigma^I}{d\Omega} = \frac{\beta\alpha^2}{4Q^2} \left[ \left| G_M^I(Q^2) \right|^2 (1 + \cos^2 \theta) + \frac{4M^2}{Q^2} \left| G_E^I(Q^2) \right|^2 \sin^2 \theta \right].$$

Here  $\beta = k/M$ ,  $Q = 2(M + E)$ , and  $\theta$  is the angle between the electron (positron) momentum  $\mathbf{P}$  and the nucleon momentum  $\mathbf{k}$ . In terms of the form factor  $G_s^I$ , the electromagnetic Sachs form factors have the form

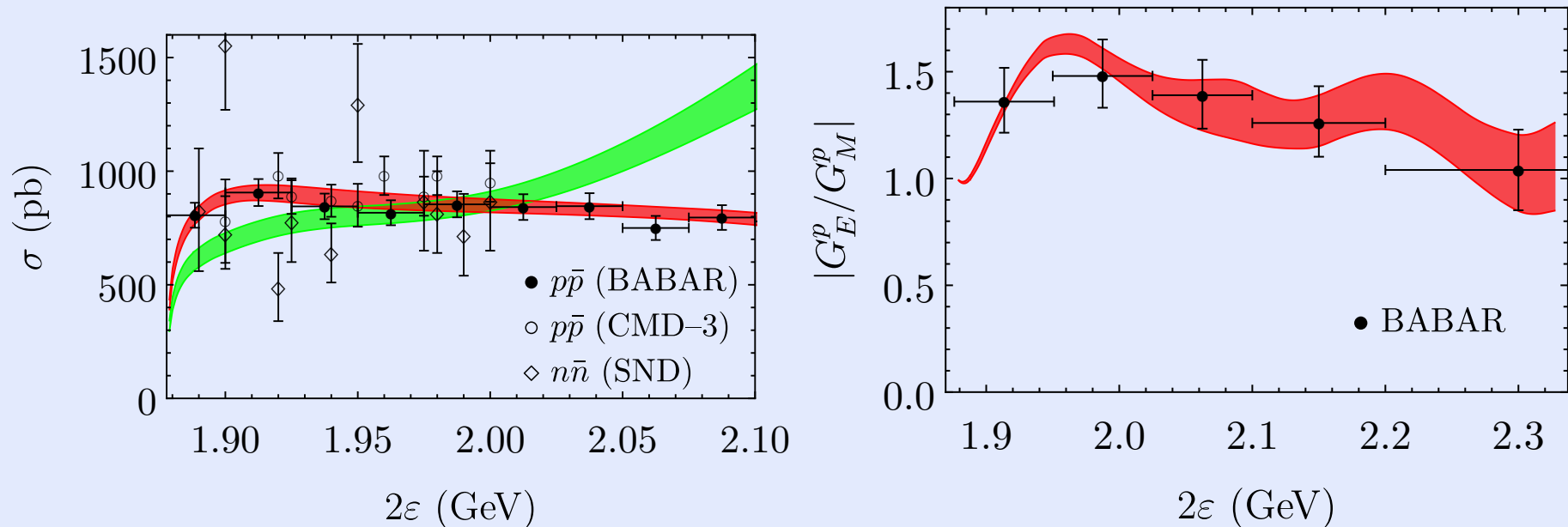
$$G_M^I = G_s^I \left[ u_{1R}^I(0) + \frac{1}{\sqrt{2}} u_{2R}^I(0) \right], \quad \frac{2M}{Q} G_E^I = G_s^I \left[ u_{1R}^I(0) - \sqrt{2} u_{2R}^I(0) \right].$$

The ratio is independent on the constant  $G_s^I$ ,

$$\frac{G_E^I}{G_M^I} = \frac{u_{1R}^I(0) - \sqrt{2} u_{2R}^I(0)}{u_{1R}^I(0) + \frac{1}{\sqrt{2}} u_{2R}^I(0)}.$$

$G_E^I/G_M^I \neq 1$  due to  $d$ -wave ( $u_{2R}^I(0) \neq 0$ )!

## Predictions for the cross section of $e^+e^- \rightarrow N\bar{N}$ near the threshold



**Left:** the cross sections of  $p\bar{p}$  (red line) and  $n\bar{n}$  (green line) production,  
**Right:**  $G_E^p/G_M^p$  for proton. The experimental data are from J.P.Lees et al., BaBar, Phys.Rev. D 87, 092005 (2013), R.R. Akhmetshin et al., CMD3, Physics Letters B759, 634 (2016) M.N. Achasov et al.,SND, Phys. Rev. D 90, 112007 (2014).

## Virtual $N\bar{N}$ pair production near the threshold.

The total cross section (elastic+inelastic)  $\sigma_{\text{tot}}^I$  can be written as (V.S.Fadin, V.A.Khoze, JETP Lett., 46, 525, (1987)):

$$\sigma_{\text{tot}}^I = -\frac{2\pi\alpha^2}{M^2Q^2} \left| G_s^I \right|^2 \text{Sp} [\text{Im} \mathcal{D} (0, 0|E)].$$

Where  $\mathcal{D}(r, r'|E)$  is the Green's function,

$$\left( \frac{p_r^2}{M} + \mathcal{V} - 2E \right) \mathcal{D} (r, r'|E) = -\frac{1}{rr'} \delta (r - r').$$

The solution of this equation has the form

$$\begin{aligned} \mathcal{D} (r, r'|E) = -Mk \sum_{n=1,2} & \left[ \vartheta (r' - r) \chi_{nR}(r) \chi_{nN}^T(r') \right. \\ & \left. + \vartheta (r - r') \chi_{nN}(r) \chi_{nR}^T(r') \right], \end{aligned}$$

where  $\chi^T$  denotes transposition of  $\chi$ .

The non-regular solutions  $\chi_{nN}(r)$  of the wave equation have the following asymptotic forms at large distances (V.F.Dmitriev, A.I.Milstein, S.G.Salnikov, Phys. Rev. D 93, 034033 (2016)):

$$u_{1N}^I(r) = \frac{1}{kr} e^{ikr}, \quad \lim_{r \rightarrow \infty} r w_{1N}^I(r) = 0,$$

$$\lim_{r \rightarrow \infty} r u_{2N}^I(r) = 0, \quad w_{2N}^I(r) = -\frac{1}{kr} e^{ikr}.$$

The inelastic cross section is the difference between the total cross section and elastic cross section:

$$\sigma_{\text{ann}}^I = \sigma_{\text{tot}}^I - \sigma^I, \quad \sigma^I = \frac{2\pi\beta\alpha^2}{Q^2} |G_s^I|^2 \left[ |u_{1R}^I(0)|^2 + |u_{2R}^I(0)|^2 \right].$$

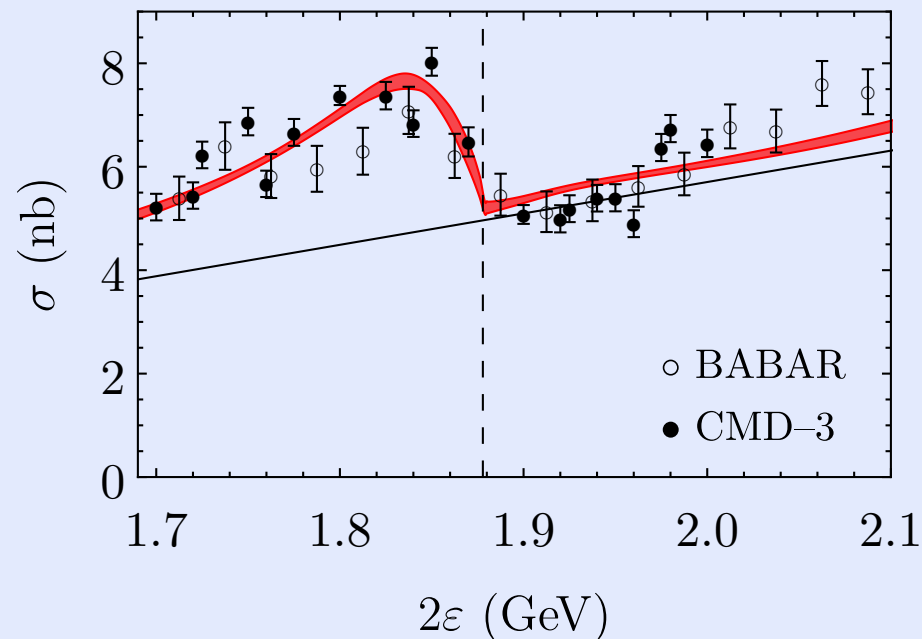
Data on  $e^+e^- \rightarrow 4\pi$  do not demonstrate strong energy dependence in the vicinity of the  $N\bar{N}$  threshold (B. Aubert et al., BaBar, Phys. Rev. D 71, 052001 (2005), M. Achasov et al., SND, EPJ Web Conf. 71, 00121 (2014)). Data on  $e^+e^- \rightarrow 5\pi$  are not accurate enough for all channels (B. Aubert et al., Phys. Rev. D 76, 092005 (2007)).

$e^+e^- \rightarrow 6\pi$  near the threshold.

The cross section in the energy region between 1.7 GeV and 2.1 GeV is approximated by the formula

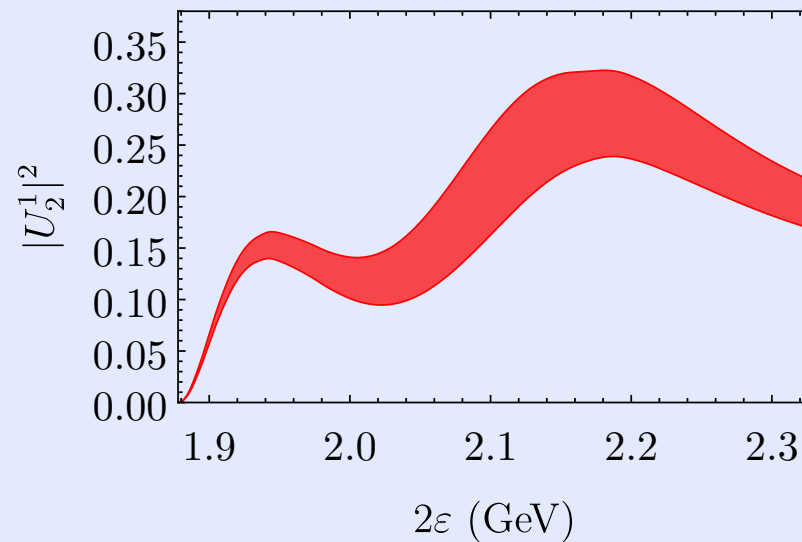
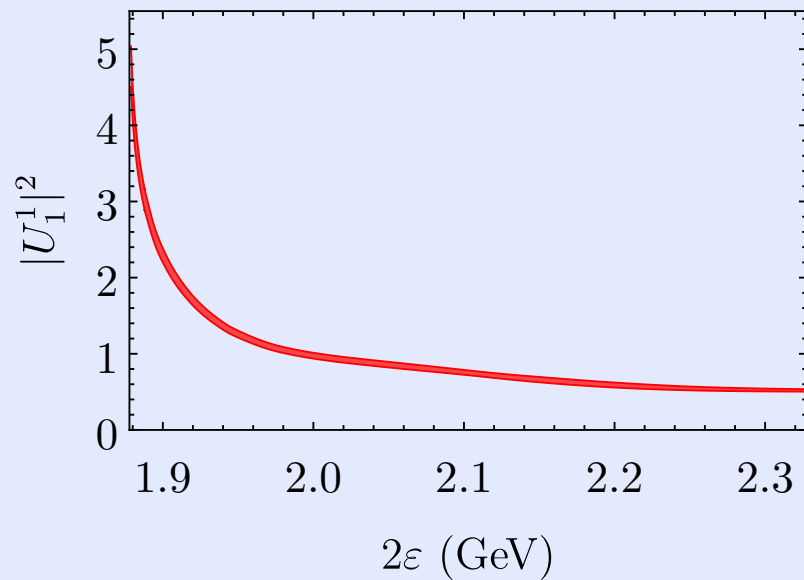
$$\sigma_{6\pi} = A\sigma_{\text{ann}}^1 + B \cdot E + C,$$

where the best coincidence is for  $A = 0.56$ ,  $B = 0.012$  nb/MeV,  $C = 4.96$  nb. The coefficient  $A$  agrees with the data of  $p\bar{p} \rightarrow \text{pions}$  annihilation at rest, where  $6\pi$  give  $\sim 55\%$  of  $I = 1$  contribution (C. Amsler et al., Nucl. Phys. A720, 357 (2003)).

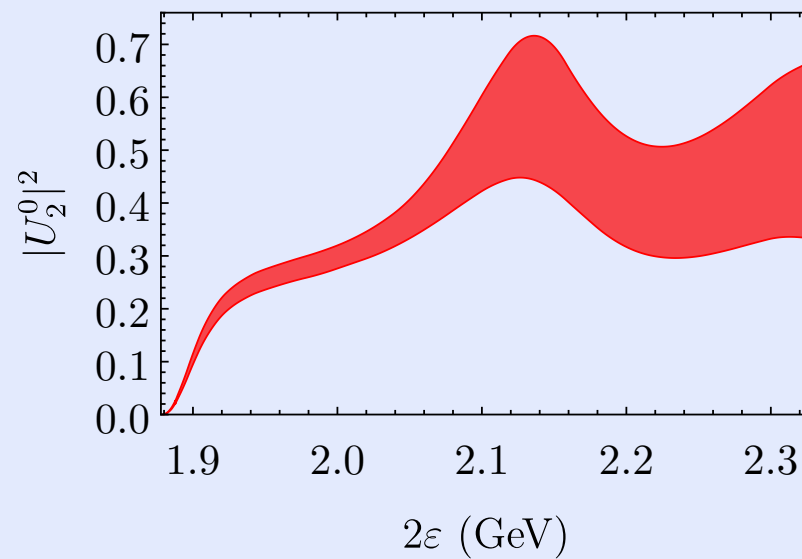
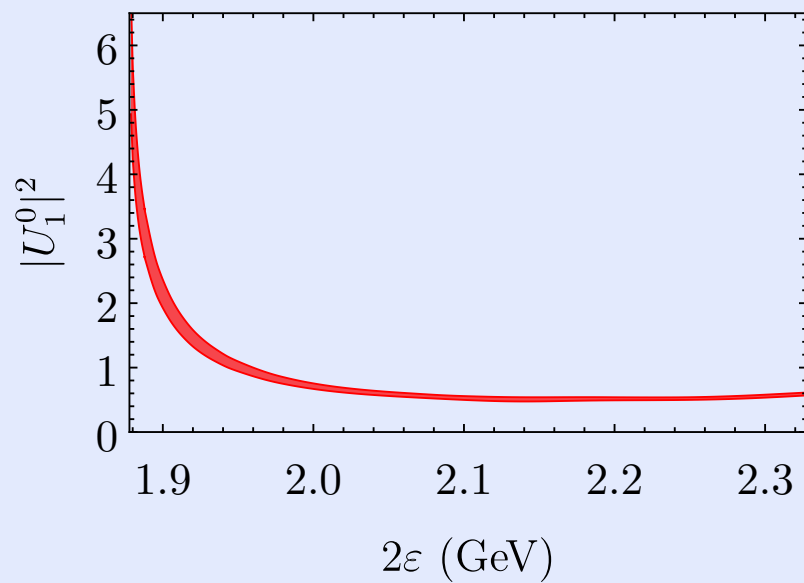


# Wave functions at origin

Isospin  $I = 1$ :



Isospin  $I = 0$ :



## Angular distributios in $J/\psi \rightarrow p\bar{p}\pi^0(\eta)$ decays

V.F.Dmitriev, A.I.Milstein, S.G.Salnikov, Phys.Lett. B760, 139 (2016)

Dominant contribution is given by the state of  $p\bar{p}$  pair with the quantum numbers  $J^{PC} = 1^{--} ({}^3S_1)$ .

Notations:  $\mathbf{k}$  is the momentum of meson in the  $J/\psi$  rest frame,  $\mathbf{p}$  is the proton momentum in the  $p\bar{p}$  center-of-mass frame,  $M$  is the invariant mass of the  $p\bar{p}$  system.

$$\frac{d\Gamma^I}{dM d\Omega_k} = \frac{\mathcal{G}_I^2 p k^3}{2^9 \pi^4 m_{J/\psi}^4} \left( \left| u_{1R}^I(0) \right|^2 + \left| u_{2R}^I(0) \right|^2 \right) \left[ 1 + \cos^2 \vartheta_k \right],$$

where  $\vartheta_k$  is the angle between  $\mathbf{n}$  and  $\mathbf{k}$ ,  $\mathbf{n}$  is directed along the electron momentum in the beam. The angular part of this distribution does not depend on the features of the  $p\bar{p}$  interaction!



The distribution over the angle  $\vartheta_p$  between  $\mathbf{p}$  and  $\mathbf{n}$ :

$$\frac{d\Gamma^I}{dM d\Omega_p} = \frac{\mathcal{G}_I^2 p k^3}{2^7 3\pi^4 m_{J/\psi}^4} \left( |u_{1R}^I(0)|^2 + |u_{2R}^I(0)|^2 \right) \left[ 1 + \gamma^I P_2(\cos \vartheta_p) \right],$$

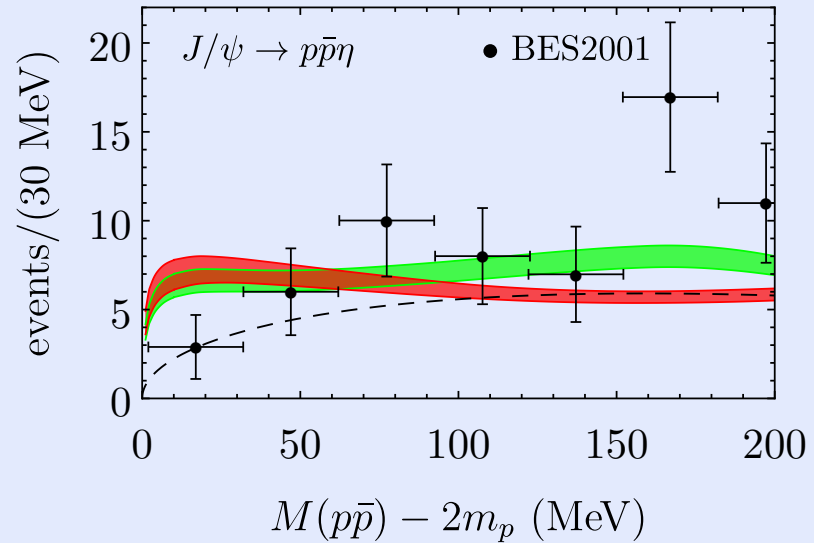
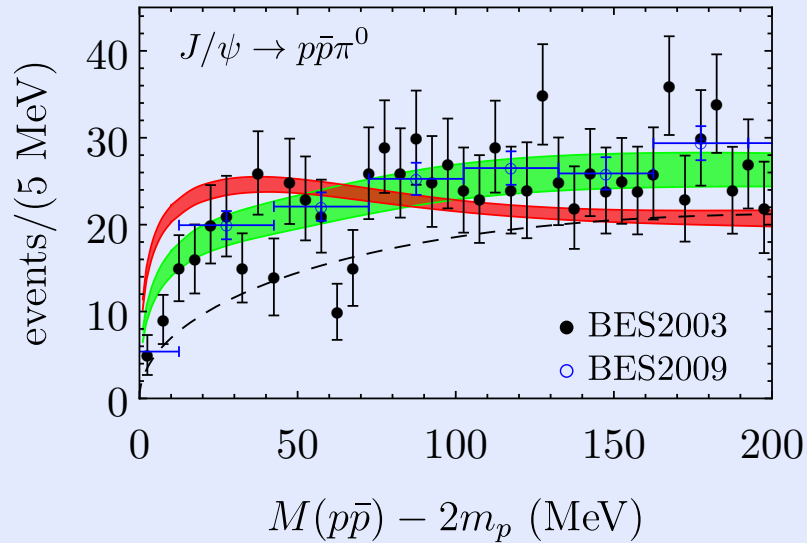
The distribution over the angle  $\vartheta_{pk}$  between  $\mathbf{p}$  and  $\mathbf{k}$ :

$$\frac{d\Gamma}{dM d\Omega_{pk}} = \frac{\mathcal{G}_I^2 p k^3}{2^7 3\pi^4 m_{J/\psi}^4} \left( |u_{1R}^I(0)|^2 + |u_{2R}^I(0)|^2 \right) \left[ 1 - 2\gamma^I P_2(\cos \vartheta_{pk}) \right].$$

where  $P_2(x) = \frac{3x^2-1}{2}$  is the Legendre polynomial,

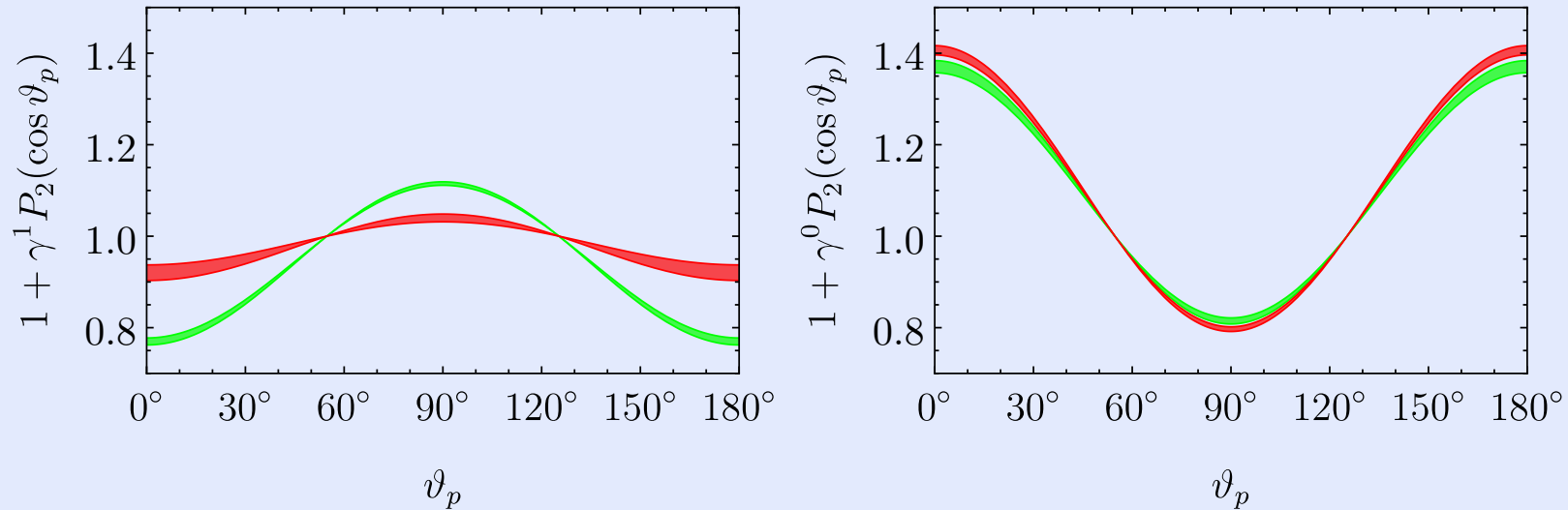
$$\gamma^I = \frac{1}{4} \frac{|u_{2R}^I(0)|^2 - 2\sqrt{2}\text{Re} [u_{1R}^I(0)u_{2R}^{I*}(0)]}{|u_{1R}^I(0)|^2 + |u_{2R}^I(0)|^2}.$$

The invariant mass spectra of  $J/\psi \rightarrow p\bar{p}\pi^0$  and  $J/\psi \rightarrow p\bar{p}\eta$  decays:

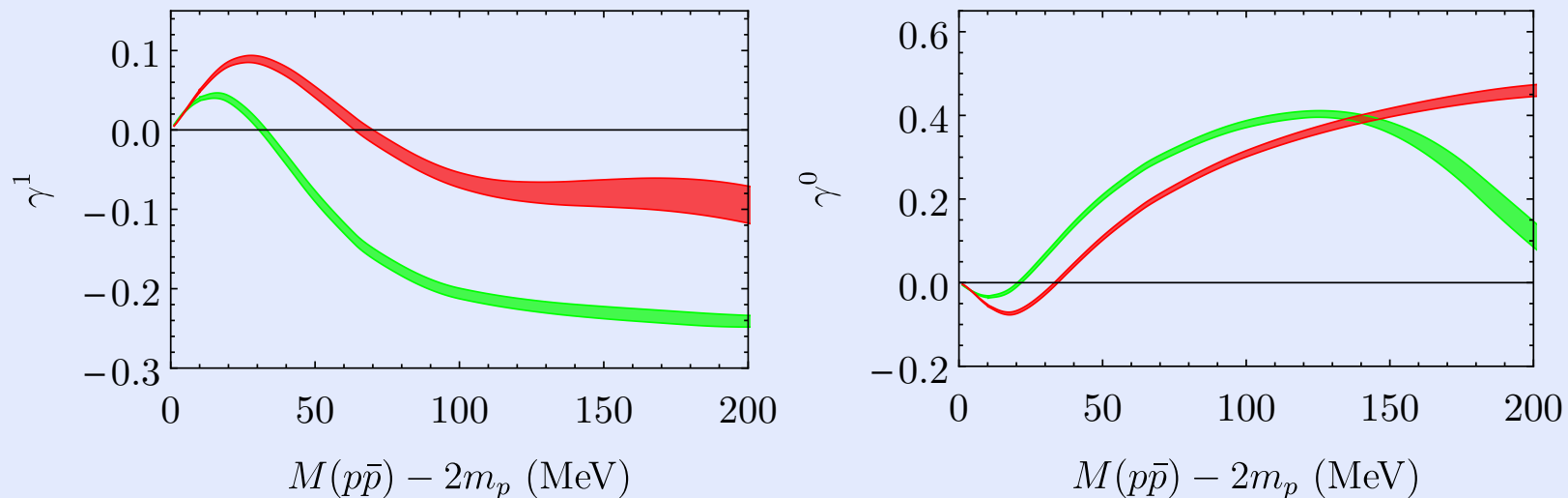


**Left:**  $J/\psi \rightarrow p\bar{p}\pi^0$  decay. **Right:**  $J/\psi \rightarrow p\bar{p}\eta$  decay. The red band corresponds to our previous parameters of the potential and the green band corresponds to the refitted model. The phase space behavior is shown by the dashed curve.

The distributions over the angle between the proton momentum and the momentum of the electrons in the beam at  $M - 2m_p = 150\text{MeV}$ :



The dependence of the anisotropy parameters  $\gamma^I$  on  $p\bar{p}$  invariant mass:



**Left:**  $J/\psi \rightarrow p\bar{p}\pi^0$  decay. **Right:**  $J/\psi \rightarrow p\bar{p}\eta$  decay.

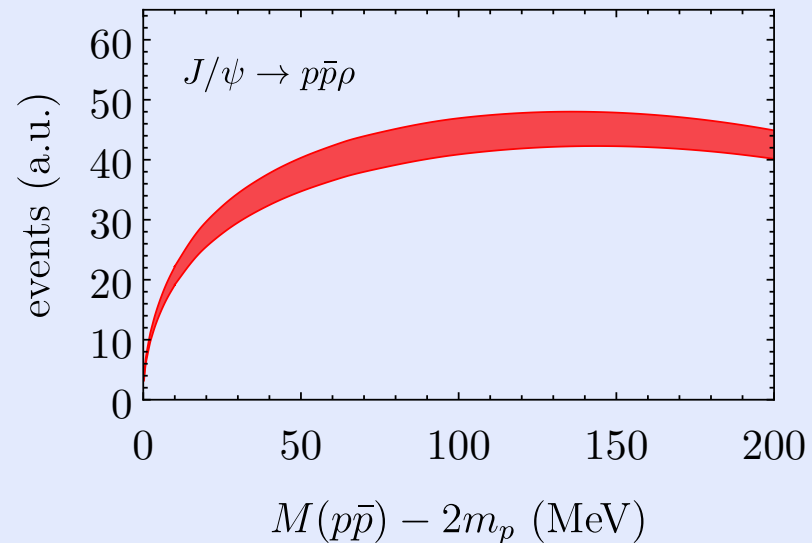
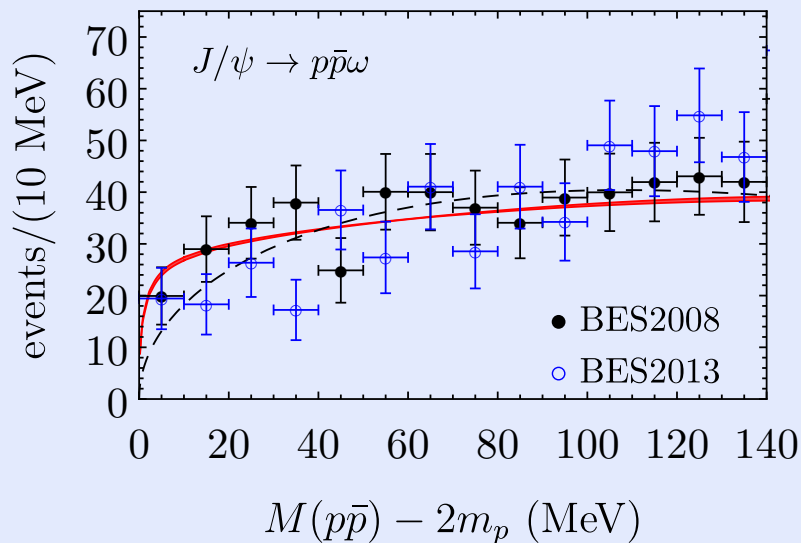
## $J/\psi \rightarrow p\bar{p}\rho(\omega)$ decays

A.I.Milstein, S.G.Salnikov, Nucl. Phys. A 966, 54 (2017)

Dominant contribution is given by the state of  $p\bar{p}$  pair with the quantum numbers  $J^{PC} = 1^{-+}$  ( $^1S_0$ ). Only one function  $u_R^I(0)$ !

$$\frac{d\Gamma^I}{dM d\Omega_p d\Omega_k} = \frac{\mathcal{G}_I^2 p k^3}{2^{10} \pi^5 m_{J/\psi}^4} \left| u_R^I(0) \right|^2 \left[ 1 + \cos^2 \vartheta_k \right],$$

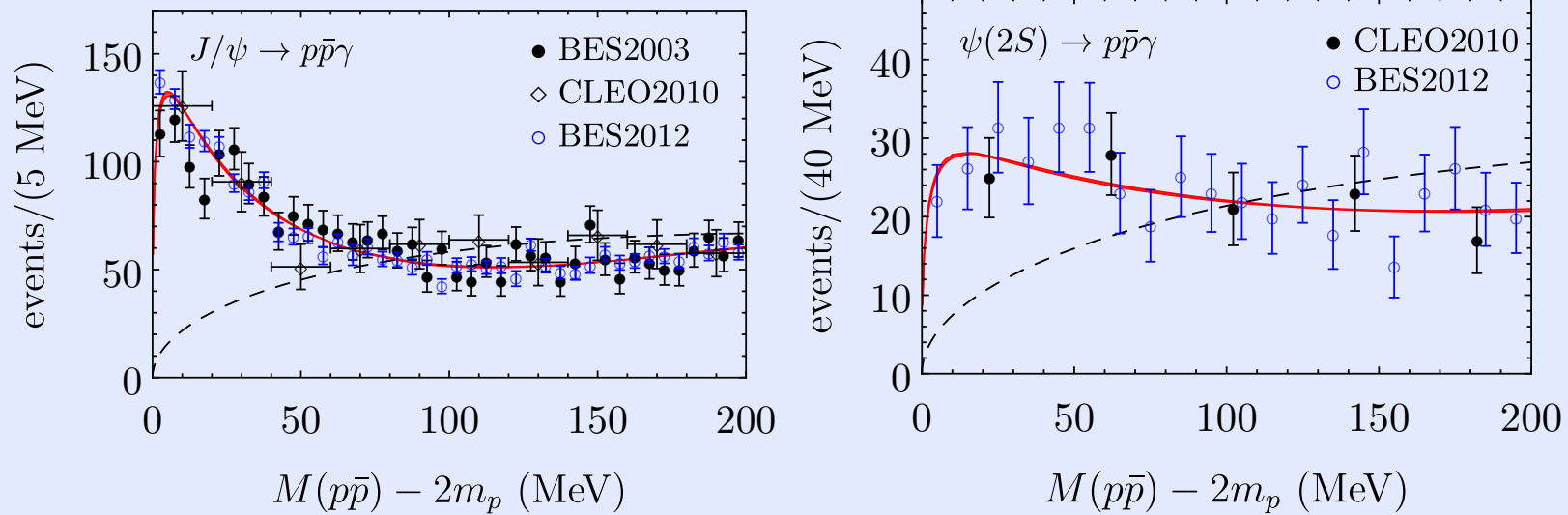
The invariant mass spectra in  $J/\psi \rightarrow p\bar{p}\rho, \omega$  decays:



**Left:**  $J/\psi \rightarrow p\bar{p}\omega$  decay. **Right:**  $J/\psi \rightarrow p\bar{p}\rho$  decay.

## $J/\psi, \psi(2S) \rightarrow p\bar{p}\gamma$ decay

The invariant mass spectra in  $J/\psi(\psi(2S)) \rightarrow p\bar{p}\gamma$  decays:



**Left:**  $J/\psi \rightarrow p\bar{p}\gamma$  decay. **Right:**  $\psi(2S) \rightarrow p\bar{p}\gamma$  decay.

$J/\psi \rightarrow \gamma\eta'\pi^+\pi^-$  decay near the  $N\bar{N}$  threshold

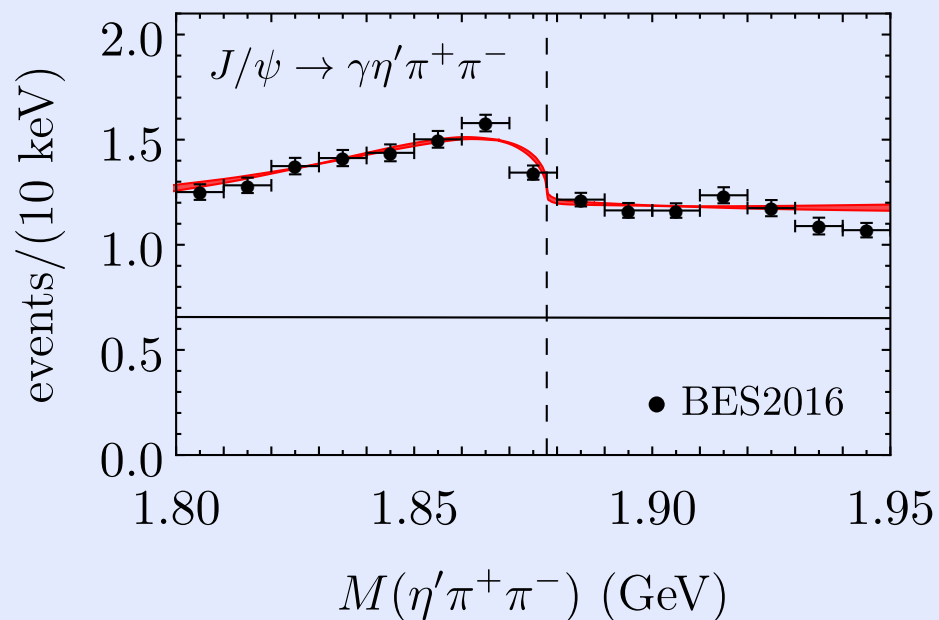
$$\frac{d\Gamma_{\text{tot}}^I}{dM} = -\frac{\mathcal{G}_I^2 k^3}{2^4 3\pi^3 m_p m_{J/\psi}^4} \text{Im}\mathcal{D}^I(0, 0|E),$$

$$d\Gamma_{\text{inel}}^I/dM = d\Gamma_{\text{tot}}^I/dM - d\Gamma_{N\bar{N}}^I/dM,$$

$$d\Gamma_{\gamma\eta'\pi^+\pi^-}/dM = Ad\Gamma_{\text{inel}}^0/dM + B \cdot E + C,$$

where  $A$ ,  $B$  and  $C$  are some fitting parameters. The coefficient  $A \approx 4 \cdot 10^{-3}$  is the estimation of the branching ratio of the decay  $p\bar{p} \rightarrow \eta'\pi^+\pi^-$  at rest. This value is very close to the branching ratio  $3.46 \cdot 10^{-3}$  measured in the experiment.

The  $\eta'\pi^+\pi^-$  invariant mass spectrum:



The thin line shows the contribution of non- $N\bar{N}$  channels. Vertical dashed line is the  $N\bar{N}$  threshold.

## Conclusion

- Unusual phenomena are related to interaction at large distances (“nuclear physics” of elementary particles).
- The results of SND and CMD-3 obtained at  $e^+e^-$  collider VEPP-2000 give an important contribution to understanding these phenomena.
- Using the data on  $e^+e^- \rightarrow N\bar{N}$  annihilation and the data on  $N\bar{N}$  scattering, we describe simultaneously: the cross section of  $e^+e^- \rightarrow \text{mesons}$ , the decays  $J/\psi \rightarrow p\bar{p}\omega$ ,  $J/\psi \rightarrow p\bar{p}\gamma$ ,  $\psi(2S) \rightarrow p\bar{p}\gamma$ ,  $J/\psi \rightarrow p\bar{p}\pi^0$ ,  $J/\psi \rightarrow p\bar{p}\eta$  and  $J/\psi \rightarrow \gamma N\bar{N} \rightarrow \gamma\eta'\pi^+\pi^-$  with good precision. We have obtained the predictions for the decay  $J/\psi \rightarrow p\bar{p}\rho$  which has not been measured yet.
- The anisotropy in the decay  $J/\psi \rightarrow p\bar{p}\pi^0$  and especially in the  $J/\psi \rightarrow p\bar{p}\eta$  decay are large enough to be measured.